Study of High Momentum ## Production in B→##X[subscript s]

Study of High Momentum η' Production in $B \to \eta' X_s$

B. Aubert,[1] R. Barate,[1] D. Boutigny,[1] F. Couderc,[1] J.-M. Gaillard,[1] A. Hicheur,[1] Y. Karyotakis,[1] J. P. Lees,[1] V. Tisserand,[1] A. Zghiche,[1] A. Palano,[2] A. Pompili,[2] J. C. Chen,[3] N. D. Qi,[3] G. Rong,[3] P. Wang,[3] Y. S. Zhu,[3] G. Eigen,[4] I. Ofte,[4] B. Stugu,[4] G. S. Abrams,[5] A.W. Borgland,[5] A. B. Breon,[5] D. N. Brown,[5] J. Button-Shafer,[5] R. N. Cahn,[5] E. Charles,[5] C.T. Day,[5] M. S. Gill,[5] A.V. Gritsan,[5] Y. Groysman,[5] R. G. Jacobsen,[5] R.W. Kadel,[5] J. Kadyk,[5] L. T. Kerth,[5] Yu. G. Kolomensky,[5] G. Kukartsev,[5] C. LeClerc,[5] M. E. Levi,[5] G. Lynch,[5] L. M. Mir,[5] P. J. Oddone,[5] T. J. Orimoto,[5] M. Pripstein,[5] N. A. Roe,[5] M.T. Ronan,[5] V. G. Shelkov,[5] A.V. Telnov,[5] W. A. Wenzel,[5] K. Ford,[6] T. J. Harrison,[6] C. M. Hawkes,[6] S. E. Morgan,[6] A. T. Watson,[6] N. K. Watson,[6] M. Fritsch,[7] K. Goetzen,[7] T. Held,[7] H. Koch,[7] B. Lewandowski,[7] M. Pelizaeus,[7] K. Peters,[7] H. Schmuecker,[7] M. Steinke,[7] J.T. Boyd,[8] N. Chevalier,[8] W. N. Cottingham,[8] M. P. Kelly,[8] T. E. Latham,[8] C. Mackay,[8] F. F. Wilson,[8] K. Abe,[9] T. Cuhadar-Donszelmann,[9] C. Hearty,[9] T. S. Mattison,[9] J. A. McKenna,[9] D. Thiessen,[9] P. Kyberd,[10] A. K. McKemey,[10] L. Teodorescu,[10] V. E. Blinov,[11] A. D. Bukin,[11] V. B. Golubev,[11] V. N. Ivanchenko,[11] E. A. Kravchenko,[11] A. P. Onuchin,[11] S. I. Serednyakov,[11] Yu. I. Skovpen,[11] E. P. Solodov,[11] A. N. Yushkov,[11] D. Best,[12] M. Bruinsma,[12] M. Chao,[12] I. Eschrich,[12] D. Kirkby,[12] A. J. Lankford,[12] M. Mandelkern,[12] R. K. Mommsen,[12] W. Roethel,[12] D. P. Stoker,[12] C. Buchanan,[13] B. L. Hartfiel,[13] J.W. Gary,[14] J. Layter,[14] B. C. Shen,[14] K. Wang,[14] D. del Re,[15] H. K. Hadavand,[15] E. J. Hill,[15] D. B. MacFarlane,[15] H. P. Paar,[15] Sh. Rahatlou,[15] V. Sharma,[15] J.W. Berryhill,[16] C. Campagnari,[16] B. Dahmes,[16] S. L. Levy,[16] O. Long,[16] A. Lu,[16] M. A. Mazur,[16] J. D. Richman,[16] W. Verkerke,[16] T.W. Beck,[17] J. Beringer,[17] A. M. Eisner,[17] C. A. Heusch,[17] W. S. Lockman,[17] T. Schalk,[17] R. E. Schmitz,[17] B. A. Schumm,[17] A. Seiden,[17] P. Spradlin,[17] W. Walkowiak,[17] D. C. Williams,[17] M. G. Wilson,[17] J. Albert,[18] E. Chen,[18] G. P. Dubois-Felsmann,[18] A. Dvoretskii,[18] R. J. Erwin,[18] D. G. Hitlin,[18] I. Narsky,[18] T. Piatenko,[18] F. C. Porter,[18] A. Ryd,[18] A. Samuel,[18] S. Yang,[18] S. Jayatilleke,[19] G. Mancinelli,[19] B. T. Meadows,[19] M. D. Sokoloff,[19] T. Abe,[20] F. Blanc,[20] P. Bloom,[20] S. Chen,[20] P. J. Clark,[20] W. T. Ford,[20] U. Nauenberg,[20] A. Olivas,[20] P. Rankin,[20] J. Roy,[20] J. G. Smith,[20] W. C. van Hoek,[20] L. Zhang,[20] J. L. Harton,[21] T. Hu,[21] A. Soffer,[21] W. H. Toki,[21] R. J. Wilson,[21] J. Zhang,[21] D. Altenburg,[22] T. Brandt,[22] J. Brose,[22] T. Colberg,[22] M. Dickopp,[22] E. Feltresi,[22] A. Hauke,[22] H. M. Lacker,[22] E. Maly,[22] R. Müller-Pfefferkorn,[22] R. Nogowski,[22] S. Otto,[22] J. Schubert,[22] K. R. Schubert,[22] R. Schwierz,[22] B. Spaan,[22] D. Bernard,[23] G. R. Bonneaud,[23] F. Brochard,[23] P. Grenier,[23] Ch. Thiebaux,[23] G. Vasileiadis,[23] M. Verderi,[23] D. J. Bard,[24] A. Khan,[24] D. Lavin,[24] F. Muheim,[24] S. Playfer,[24] M. Andreotti,[25] V. Azzolini,[25] D. Bettoni,[25] C. Bozzi,[25] R. Calabrese,[25] G. Cibinetto,[25] E. Luppi,[25] M. Negrini,[25] L. Piemontese,[25] A. Sarti,[25] E. Treadwell,[26] R. Baldini-Ferroli,[27] A. Calcaterra,[27] R. de Sangro,[27] G. Finocchiaro,[27] P. Patteri,[27] M. Piccolo,[27] A. Zallo,[27] A. Buzzo,[28] R. Capra,[28] R. Contri,[28] G. Crosetti,[28] M. Lo Vetere,[28] M. Macri,[28] M. R. Monge,[28] S. Passaggio,[28] C. Patrignani,[28] E. Robutti,[28] A. Santroni,[28] S. Tosi,[28] S. Bailey,[29] M. Morii,[29] E. Won,[29] R. S. Dubitzky,[30] U. Langenegger,[30] W. Bhimji,[31] D. A. Bowerman,[31] P. D. Dauncey,[31] U. Egede,[31] J. R. Gaillard,[31] G.W. Morton,[31] J. A. Nash,[31] G. P. Taylor,[31] G. J. Grenier,[32] S.-J. Lee,[32] U. Mallik,[32] J. Cochran,[33] H. B. Crawley,[33] J. Lamsa,[33] W. T. Meyer,[33] S. Prell,[33] E. I. Rosenberg,[33] J. Yi,[33] M. Davier,[34] G. Grosdidier,[34] A. Höcker,[34] S. Laplace,[34] F. Le Diberder,[34] V. Lepeltier,[34] A. M. Lutz,[34] T. C. Petersen,[34] S. Plaszczynski,[34] M. H. Schune,[34] L. Tantot,[34] G. Wormser,[34] V. Brigljević,[35] C. H. Cheng,[35] D. J. Lange,[35] M. C. Simani,[35] D. M. Wright,[35] A. J. Bevan,[36] J. P. Coleman,[36] J. R. Fry,[36] E. Gabathuler,[36] R. Gamet,[36] M. Kay,[36] R. J. Parry,[36] D. J. Payne,[36] R. J. Sloane,[36] C. Touramanis,[36] J. J. Back,[37] P. F. Harrison,[37] G. B. Mohanty,[37] C. L. Brown,[38] G. Cowan,[38] R. L. Flack,[38] H. U. Flaecher,[38] S. George,[38] M. G. Green,[38] A. Kurup,[38] C. E. Marker,[38] T. R. McMahon,[38] S. Ricciardi,[38] F. Salvatore,[38] G. Vaitsas,[38] M. A. Winter,[38] D. Brown,[39] C. L. Davis,[39] J. Allison,[40] N. R. Barlow,[40] R. J. Barlow,[40] P. A. Hart,[40] M. C. Hodgkinson,[40] G. D. Lafferty,[40] A. J. Lyon,[40] J. C. Williams,[40] A. Farbin,[41] W. D. Hulsbergen,[41] A. Jawahery,[41] D. Kovalskyi,[41] C. K. Lae,[41] V. Lillard,[41] D. A. Roberts,[41] G. Blaylock,[42] C. Dallapiccola,[42] K. T. Flood,[42] S. S. Hertzbach,[42] R. Kofler,[42] V. B. Koptchev,[42] T. B. Moore,[42] S. Saremi,[42] H. Staengle,[42] S. Willocq,[42] R. Cowan,[43] G. Sciolla,[43] F. Taylor,[43] R. K. Yamamoto,[43] D. J. J. Mangeol,[44] P. M. Patel,[44] S. H. Robertson,[44] A. Lazzaro,[45] F. Palombo,[45] J. M. Bauer,[46] L. Cremaldi,[46] V. Eschenburg,[46] R. Godang,[46] R. Kroeger,[46] J. Reidy,[46] D. A. Sanders,[46] D. J. Summers,[46] H.W. Zhao,[46] S. Brunet,[47] D. Cote-Ahern,[47] P. Taras,[47] H. Nicholson,[48] C. Cartaro,[49] N. Cavallo,[49] G. De Nardo,[49] F. Fabozzi,[49,*] C. Gatto,[49] L. Lista,[49] P. Paolucci,[49] D. Piccolo,[49] C. Sciacca,[49] M. A. Baak,[50] G. Raven,[50] L. Wilden,[50] C. P. Jessop,[51] J. M. LoSecco,[51] T. A. Gabriel,[52] T. Allmendinger,[53] B. Brau,[53] K. K. Gan,[53] K. Honscheid,[53] D. Hufnagel,[53] H. Kagan,[53] R. Kass,[53] T. Pulliam,[53] R. Ter-Antonyan,[53] Q. K. Wong,[53] J. Brau,[54] R. Frey,[54] O. Igonkina,[54] C. T. Potter,[54] N. B. Sinev,[54] D. Strom,[54]

E. Torrence,[54] F. Colecchia,[55] A. Dorigo,[55] F. Galeazzi,[55] M. Margoni,[55] M. Morandin,[55] M. Posocco,[55] M. Rotondo,[55] F. Simonetto,[55] R. Stroili,[55] G. Tiozzo,[55] C. Voci,[55] M. Benayoun,[56] H. Briand,[56] J. Chauveau,[56] P. David,[56] Ch. de la Vaissière,[56] L. Del Buono,[56] O. Hamon,[56] M. J. J. John,[56] Ph. Leruste,[56] J. Ocariz,[56] M. Pivk,[56] L. Roos,[56] S. T'Jampens,[56] G. Therin,[56] P. F. Manfredi,[57] V. Re,[57] P. K. Behera,[58] L. Gladney,[58] Q. H. Guo,[58] J. Panetta,[58] F. Anulli,[27,59] M. Biasini,[59] I. M. Peruzzi,[27,59] M. Pioppi,[59] C. Angelini,[60] G. Batignani,[60] S. Bettarini,[60] M. Bondioli,[60] F. Bucci,[60] G. Calderini,[60] M. Carpinelli,[60] V. Del Gamba,[60] F. Forti,[60] M. A. Giorgi,[60] A. Lusiani,[60] G. Marchiori,[60] F. Martinez-Vidal,[60,†] M. Morganti,[60] N. Neri,[60] E. Paoloni,[60] M. Rama,[60] G. Rizzo,[60] F. Sandrelli,[60] J. Walsh,[60] M. Haire,[61] D. Judd,[61] K. Paick,[61] D. E. Wagoner,[61] N. Danielson,[62] P. Elmer,[62] C. Lu,[62] V. Miftakov,[62] J. Olsen,[62] A. J. S. Smith,[62] E. W. Varnes,[62] F. Bellini,[63] G. Cavoto,[62,63] R. Faccini,[63] F. Ferrarotto,[63] F. Ferroni,[63] M. Gaspero,[63] M. A. Mazzoni,[63] S. Morganti,[63] M. Pierini,[63] G. Piredda,[63] F. Safai Tehrani,[63] C. Voena,[63] S. Christ,[64] G. Wagner,[64] R. Waldi,[64] T. Adye,[65] N. De Groot,[65] B. Franek,[65] N. I. Geddes,[65] G. P. Gopal,[65] E. O. Olaiya,[65] S. M. Xella,[65] R. Aleksan,[66] S. Emery,[66] A. Gaidot,[66] S. F. Ganzhur,[66] P.-F. Giraud,[66] G. Hamel de Monchenault,[66] W. Kozanecki,[66] M. Langer,[66] M. Legendre,[66] G. W. London,[66] B. Mayer,[66] G. Schott,[66] G. Vasseur,[66] Ch. Yeche,[66] M. Zito,[66] M. V. Purohit,[67] A. W. Weidemann,[67] F. X. Yumiceva,[67] D. Aston,[68] R. Bartoldus,[68] N. Berger,[68] A. M. Boyarski,[68] O. L. Buchmueller,[68] M. R. Convery,[68] M. Cristinziani,[68] D. Dong,[68] J. Dorfan,[68] D. Dujmic,[68] W. Dunwoodie,[68] E. E. Elsen,[68] R. C. Field,[68] T. Glanzman,[68] S. J. Gowdy,[68] T. Hadig,[68] V. Halyo,[68] T. Hryn'ova,[68] W. R. Innes,[68] M. H. Kelsey,[68] P. Kim,[68] M. L. Kocian,[68] D. W. G. S. Leith,[68] J. Libby,[68] S. Luitz,[68] V. Luth,[68] H. L. Lynch,[68] H. Marsiske,[68] R. Messner,[68] D. R. Muller,[68] C. P. O'Grady,[68] V. E. Ozcan,[68] A. Perazzo,[68] M. Perl,[68] S. Petrak,[68] B. N. Ratcliff,[68] A. Roodman,[68] A. A. Salnikov,[68] R. H. Schindler,[68] J. Schwiening,[68] G. Simi,[68] A. Snyder,[68] A. Soha,[68] J. Stelzer,[68] D. Su,[68] M. K. Sullivan,[68] J. Va'vra,[68] S. R. Wagner,[68] M. Weaver,[68] A. J. R. Weinstein,[68] W. J. Wisniewski,[68] D. H. Wright,[68] C. C. Young,[68] P. R. Burchat,[69] A. J. Edwards,[69] T. I. Meyer,[69] B. A. Petersen,[69] C. Roat,[69] M. Ahmed,[70] S. Ahmed,[70] M. S. Alam,[70] J. A. Ernst,[70] M. A. Saeed,[70] M. Saleem,[70] F. R. Wappler,[70] W. Bugg,[71] M. Krishnamurthy,[71] S. M. Spanier,[71] R. Eckmann,[72] H. Kim,[72] J. L. Ritchie,[72] A. Satpathy,[72] R. F. Schwitters,[72] J. M. Izen,[73] I. Kitayama,[73] X. C. Lou,[73] S. Ye,[73] F. Bianchi,[74] M. Bona,[74] F. Gallo,[74] D. Gamba,[74] C. Borean,[75] L. Bosisio,[75] F. Cossutti,[75] G. Della Ricca,[75] S. Dittongo,[75] S. Grancagnolo,[75] L. Lanceri,[75] P. Poropat,[75,‡] L. Vitale,[75] G. Vuagnin,[75] R. S. Panvini,[76] Sw. Banerjee,[77] C. M. Brown,[77] D. Fortin,[77] P. D. Jackson,[77] R. Kowalewski,[77] J. M. Roney,[77] H. R. Band,[78] S. Dasu,[78] M. Datta,[78] A. M. Eichenbaum,[78] J. R. Johnson,[78] P. E. Kutter,[78] H. Li,[78] R. Liu,[78] F. Di Lodovico,[78] A. Mihalyi,[78] A. K. Mohapatra,[78] Y. Pan,[78] R. Prepost,[78] S. J. Sekula,[78] J. H. von Wimmersperg-Toeller,[78] J. Wu,[78] S. L. Wu,[78] Z. Yu,[78] and H. Neal[79]

(*BABAR* Collaboration)

[1]*Laboratoire de Physique des Particules, F-74941 Annecy-le-Vieux, France*
[2]*Università di Bari, Dipartimento di Fisica and INFN, I-70126 Bari, Italy*
[3]*Institute of High Energy Physics, Beijing 100039, China*
[4]*University of Bergen, Institute of Physics, N-5007 Bergen, Norway*
[5]*Lawrence Berkeley National Laboratory and University of California, Berkeley, California 94720, USA*
[6]*University of Birmingham, Birmingham, B15 2TT, United Kingdom*
[7]*Ruhr Universität Bochum, Institut für Experimentalphysik 1, D-44780 Bochum, Germany*
[8]*University of Bristol, Bristol BS8 1TL, United Kingdom*
[9]*University of British Columbia, Vancouver, British Columbia, Canada V6T 1Z1*
[10]*Brunel University, Uxbridge, Middlesex UB8 3PH, United Kingdom*
[11]*Budker Institute of Nuclear Physics, Novosibirsk 630090, Russia*
[12]*University of California at Irvine, Irvine, California 92697, USA*
[13]*University of California at Los Angeles, Los Angeles, California 90024, USA*
[14]*University of California at Riverside, Riverside, California 92521, USA*
[15]*University of California at San Diego, La Jolla, California 92093, USA*
[16]*University of California at Santa Barbara, Santa Barbara, California 93106, USA*
[17]*University of California at Santa Cruz, Institute for Particle Physics, Santa Cruz, California 95064, USA*
[18]*California Institute of Technology, Pasadena, California 91125, USA*
[19]*University of Cincinnati, Cincinnati, Ohio 45221, USA*
[20]*University of Colorado, Boulder, Colorado 80309, USA*
[21]*Colorado State University, Fort Collins, Colorado 80523, USA*
[22]*Technische Universität Dresden, Institut für Kern- und Teilchenphysik, D-01062 Dresden, Germany*
[23]*Ecole Polytechnique, LLR, F-91128 Palaiseau, France*
[24]*University of Edinburgh, Edinburgh EH9 3JZ, United Kingdom*

[25]Università di Ferrara, Dipartimento di Fisica and INFN, I-44100 Ferrara, Italy
[26]Florida A&M University, Tallahassee, Florida 32307, USA
[27]Laboratori Nazionali di Frascati dell'INFN, I-00044 Frascati, Italy
[28]Università di Genova, Dipartimento di Fisica and INFN, I-16146 Genova, Italy
[29]Harvard University, Cambridge, Massachusetts 02138, USA
[30]Universität Heidelberg, Physikalisches Institut, Philosophenweg 12, D-69120 Heidelberg, Germany
[31]Imperial College London, London SW7 2AZ, United Kingdom
[32]University of Iowa, Iowa City, Iowa 52242, USA
[33]Iowa State University, Ames, Iowa 50011-3160, USA
[34]Laboratoire de l'Accélérateur Linéaire, F-91898 Orsay, France
[35]Lawrence Livermore National Laboratory, Livermore, California 94550, USA
[36]University of Liverpool, Liverpool L69 3BX, United Kingdom
[37]Queen Mary, University of London, London E1 4NS, United Kingdom
[38]University of London, Royal Holloway and Bedford New College, Egham, Surrey TW20 0EX, United Kingdom
[39]University of Louisville, Louisville, Kentucky 40292, USA
[40]University of Manchester, Manchester M13 9PL, United Kingdom
[41]University of Maryland, College Park, Maryland 20742, USA
[42]University of Massachusetts, Amherst, Massachusetts 01003, USA
[43]Massachusetts Institute of Technology, Laboratory for Nuclear Science, Cambridge, Massachusetts 02139, USA
[44]McGill University, Montréal, Quebec, Canada H3A 2T8
[45]Università di Milano, Dipartimento di Fisica and INFN, I-20133 Milano, Italy
[46]University of Mississippi, University, Mississippi 38677, USA
[47]Université de Montréal, Laboratoire René J. A. Lévesque, Montréal, Quebec, Canada H3C 3J7
[48]Mount Holyoke College, South Hadley, Massachusetts 01075, USA
[49]Università di Napoli Federico II, Dipartimento di Scienze Fisiche and INFN, I-80126, Napoli, Italy
[50]NIKHEF, National Institute for Nuclear Physics and High Energy Physics, NL-1009 DB Amsterdam, The Netherlands
[51]University of Notre Dame, Notre Dame, Indiana 46556, USA
[52]Oak Ridge National Laboratory, Oak Ridge, Tennessee 37831, USA
[53]The Ohio State University, Columbus, Ohio 43210, USA
[54]University of Oregon, Eugene, Oregon 97403, USA
[55]Università di Padova, Dipartimento di Fisica and INFN, I-35131 Padova, Italy
[56]Universités Paris VI et VII, Lab de Physique Nucléaire H. E., F-75252 Paris, France
[57]Università di Pavia, Dipartimento di Elettronica and INFN, I-27100 Pavia, Italy
[58]University of Pennsylvania, Philadelphia, Pennsylvania 19104, USA
[59]Università di Perugia, Dipartimento di Fisica and INFN, I-06100 Perugia, Italy
[60]Università di Pisa, Dipartimento di Fisica, Scuola Normale Superiore and INFN, I-56127 Pisa, Italy
[61]Prairie View A&M University, Prairie View, Texas 77446, USA
[62]Princeton University, Princeton, New Jersey 08544, USA
[63]Università di Roma La Sapienza, Dipartimento di Fisica and INFN, I-00185 Roma, Italy
[64]Universität Rostock, D-18051 Rostock, Germany
[65]Rutherford Appleton Laboratory, Chilton, Didcot, Oxon OX11 0QX, United Kingdom
[66]DSM/Dapnia, CEA/Saclay, F-91191 Gif-sur-Yvette, France
[67]University of South Carolina, Columbia, South Carolina 29208, USA
[68]Stanford Linear Accelerator Center, Stanford, California 94309, USA
[69]Stanford University, Stanford, California 94305-4060, USA
[70]State University of New York, Albany, New York 12222, USA
[71]University of Tennessee, Knoxville, Tennessee 37996, USA
[72]University of Texas at Austin, Austin, Texas 78712, USA
[73]University of Texas at Dallas, Richardson, Texas 75083, USA
[74]Università di Torino, Dipartimento di Fisica Sperimentale and INFN, I-10125 Torino, Italy
[75]Università di Trieste, Dipartimento di Fisica and INFN, I-34127 Trieste, Italy
[76]Vanderbilt University, Nashville, Tennessee 37235, USA
[77]University of Victoria, Victoria, British Columbia, Canada V8W 3P6
[78]University of Wisconsin, Madison, Wisconsin 53706, USA
[79]Yale University, New Haven, Connecticut 06511, USA

(Received 28 December 2003; published 3 August 2004)

We measure the branching fraction for the charmless semi-inclusive process $B \to \eta' X_s$, where the η' meson has a momentum in the range 2.0 to 2.7 GeV/c in the $\Upsilon(4S)$ center-of-mass frame and X_s represents a system comprising a kaon and zero to four pions. We find $\mathcal{B}(B \to \eta' X_s) = [3.9 \pm 0.8(\text{stat}) \pm 0.5(\text{syst}) \pm 0.8(\text{model})] \times 10^{-4}$. We also obtain the X_s mass spectrum and find that it fits models predicting high masses.

DOI: 10.1103/PhysRevLett.93.061801 PACS numbers: 13.25.Hw, 13.66.Bc, 14.40.Nd

The production of high momentum η' mesons in B meson decays is expected to be dominated by the $B \to \eta' X_s$ process, where X_s is a strange hadronic system, generated by the $b \to sg^*$ transition as depicted in Figs. 1(a)–1(c). Figure 1(d) shows the color-suppressed modes $\overline{B}^0 \to \eta' D^{(*)0}$, which are significant sources of background and which have been measured for the first time recently [1]. Contributions from $b \to u$ transitions and other sources of η' are expected to be negligible [2].

The large inclusive η' production branching fraction measured by the CLEO Collaboration [3] prompted intense theoretical activity, which focused the special character of the η' meson as receiving much of its mass from the QCD anomaly [4–6]. A later measurement by CLEO confirmed the large η' production, measuring $\mathcal{B}(B \to \eta' X_{nc}) = [4.6 \pm 1.1(\text{stat}) \pm 0.4(\text{syst}) \pm 0.5(\text{bkg})] \times 10^{-4}$ [7], where X_{nc} denotes a charmless recoiling hadronic system including X_s.

We present results for the branching fraction of $B \to \eta' X_s$ and the fully background-subtracted mass spectrum of X_s. The signal is analyzed for η' momentum between 2.0 and 2.7 GeV/c in the center-of-mass (c.m.) frame to suppress background coming from $b \to c \to \eta'$ cascades such as $B \to D_s X$ with $D_s \to \eta' X$, $B \to DX$ with $D \to \eta' X$, $B \to \Lambda_c X$ with $\Lambda_c \to \eta' X$. The improvement of the measurement, based on a better background suppression and the tagging of the strangeness of the recoiling hadronic mass can provide important clues to the dynamics of the transition $b \to sg^*$ and to the structure of the isosinglet pseudoscalar mesons.

Our analysis is based on data collected with the *BABAR* detector [8] at the PEP-II asymmetric e^+e^- collider located at the Stanford Linear Accelerator Center. An integrated luminosity of 81.4 fb^{-1}, corresponding to 88.4×10^6 $B\overline{B}$ pairs, was recorded at the $\Upsilon(4S)$ resonance (on-resonance) and 9.6 fb^{-1} were recorded 40 MeV below this resonance (off-resonance), for continuum background studies.

Two tracking devices are used for the detection of charged particles: a silicon vertex tracker consisting of five layers of double-sided silicon microstrip detectors, and a 40-layer central drift chamber, both operating in the 1.5 T magnetic field of a superconducting solenoid. Photons and electrons are detected by a CsI(Tl) electromagnetic calorimeter. Charged-particle identification is provided by the average energy loss (dE/dx) in the tracking devices, and by an internally reflecting ring-imaging Cherenkov detector covering the central region.

We select $B\overline{B}$ events by requiring at least four charged tracks and a value of the ratio of the second to zeroth Fox-Wolfram moment [9] less than 0.5. We form a B candidate by combining an $\eta' \to \eta\pi^+\pi^-$, where the η decays into $\gamma\gamma$, with a K^+ or a K^0_S that is reconstructed in the $\pi^+\pi^-$ channel, and up to four pions, of which at most one is a π^0, leading to 16 possible channels [10]:

$$
\begin{aligned}
&B^+ \to \eta' K^+(+\pi^0) && B^0 \to \eta' K^0_S(+\pi^0),\\
&B^+ \to \eta' K^+\pi^+\pi^-(+\pi^0) && B^0 \to \eta' K^0_S\pi^+\pi^-(+\pi^0),\\
&B^+ \to \eta' K^0_S\pi^+(+\pi^0) && B^0 \to \eta' K^+\pi^-(+\pi^0),\\
&B^+ \to \eta' K^0_S\pi^+\pi^+\pi^-(+\pi^0) && B^0 \to \eta' K^+\pi^-\pi^+\pi^-(+\pi^0).
\end{aligned}
$$

The masses of the $\eta \to \gamma\gamma$, $K^0_S \to \pi^+\pi^-$, and $\pi^0 \to \gamma\gamma$ candidates are required to lie within 3σ ($\sigma = 16$, 3, and 6 MeV/c^2, respectively) of their known values and are then kinematically constrained to their nominal masses.

To identify the s quark in the X_s system, we require a K^0_S or a track consistent with a charged kaon. The charged-kaon selection has been optimized to suppress background from $B \to \eta'\pi$, $\eta'\rho$, and $\eta' a_1$ decays. For the K^0_S, we require the angle α between the momentum of the K^0_S candidate and its flight direction to be less than 0.05 radians, as it peaks at zero for true K^0_S particles.

We require candidates for $B \to \eta' X_s$ to be consistent with a B decay, based on the beam-energy-substituted mass $m_{\text{ES}} = \sqrt{(s/2 + \mathbf{p}_0 \cdot \mathbf{p}_B)^2/E_0^2 - \mathbf{p}_B^2}$ and the energy

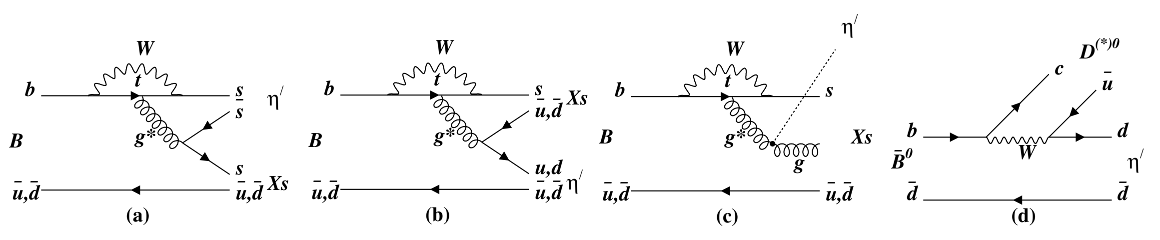

FIG. 1. Lowest order diagrams for (a)–(c) $B \to \eta' X_s$ and (d) the color-suppressed background $\overline{B}^0 \to \eta' D^{(*)0}$.

difference $\Delta E = E_B^* - \sqrt{s}/2$, where E and $\mathbf{p}$ denote the energy and momentum of the particles, the subscripts 0 and B refer to the initial $\Upsilon(4S)$ and the B candidate, respectively, the asterisk denotes the $\Upsilon(4S)$ rest frame, and $\sqrt{s}$ is the e^+e^- c.m. energy [11]. In addition, the cosine of the angle between the thrust axis of the B candidate and that of the rest of the event in the c.m. frame ($\cos\theta_T^*$) is used to remove continuum background, which is peaked near $|\cos\theta_T^*| = 1$, while signal events are uniformly distributed. We require $m_{\rm ES} > 5.265$ GeV$/c^2$, $|\Delta E| < 0.1$ GeV, and $|\cos\theta_T^*| < 0.8$. For each event, we select the candidate with the smallest χ^2, with χ^2 defined by

$$\chi^2 = (m_{\rm ES} - M_B)^2/\sigma^2(m_{\rm ES}) + (\Delta E)^2/\sigma^2(\Delta E),$$

where M_B is the B-meson mass and where the resolutions $\sigma(m_{\rm ES}) = 3$ MeV$/c^2$ and $\sigma(\Delta E) = 25$ MeV are obtained from Monte Carlo simulation. The remaining continuum background is subtracted with the use of off-resonance data.

The background contribution from color-suppressed modes $\overline{B}^0 \to \eta' D^{(*)0}$ is estimated from a Monte Carlo simulation which uses our measurement of its branching fraction, $\mathcal{B}(\overline{B}^0 \to \eta' D^{(*)0}) = [1.7 \pm 0.4(\text{stat}) \pm 0.2(\text{syst})] \times 10^{-4}$ [1].

To determine efficiencies, we model the signal using a combination of the two-body mode $B \to \eta' K$ and, for X_s masses above the $K\pi$ threshold, a nonresonant hard spectrum derived from the theoretical predictions [4–6], which are based on the anomalous η'-gluon-gluon coupling and which favor high-mass X_s systems. The fraction of the two-body mode is constrained in the simulation model to be between 10% and 15% [12,13]. When not forming a K meson, the X_s fragments into $s\bar{q}$ and $s\bar{q}g$ ($q = u, d$). We find that the overall efficiency is $(6.0 \pm 0.2)\%$ for the $K^\pm$ modes and $(4.7 \pm 0.1)\%$ for the K_S^0 modes, including the branching fraction $\mathcal{B}(K_S^0 \to \pi^+\pi^-)$.

The branching fraction of $B \to \eta' X_s$ is computed through a fit to the number of η' signal events, with η' momentum between 2.0 and 2.7 GeV$/c$, both for on-resonance and off-resonance data. To parametrize the background, we use a Gaussian function for the signal and a second order polynomial. For the fit of the off-resonance data sample, we constrain the mass and width of the η' to the values obtained with on-resonance data. Figure 2 shows the fits of the $\eta\pi\pi$ invariant-mass distributions for the $K^\pm$ and K_S^0 modes. The fitted yields are reported in Table I.

The semi-inclusive branching fraction is computed by performing a weighted average of the results obtained for the $K^\pm$ and K_S^0 modes. The detection efficiencies are corrected to account for the η' and η branching fractions to the channel we observe. For the K_S^0 modes, we convert the result so it corresponds to K^0 and $\overline{K}^0$. The final state X_s includes both K^+- and K^0-tagged decays. Assuming that their branching fractions are equal, we obtain $\mathcal{B}(B \to \eta' X_s) = [3.9 \pm 0.8(\text{stat}) \pm 0.5(\text{syst}) \pm 0.8(\text{model})] \times 10^{-4}$. We obtain the systematic error by combining the sources listed in Table II; of the total error 8% is common to all the $\eta' K n\pi$ combinations.

TABLE I. Results of the fits for $K^\pm$ and K_S^0 modes. Yields for on-resonance data ($Y_{\rm ON}$), off-resonance data ($Y_{\rm OFF}$), expectation from color-suppressed background ($Y_{\rm CS}$) and on-resonance data after background subtraction (Y) are given. A luminosity scale factor, $f = 8.48$, is applied to the off-resonance yield.

	$K^\pm$ modes	K_S^0 modes
$Y_{\rm ON}$	577.0 ± 34.0	367.0 ± 34.0
$Y_{\rm OFF}$	18.9 ± 8.5	21.7 ± 8.4
$Y_{\rm CS}$	63.6 ± 11.4	26.9 ± 4.5
Y	353.1 ± 80.5	156.1 ± 79.1

The largest uncertainty arises from our model of the X_s system. To estimate that uncertainty, we use an alternative model which consists of a combination of resonant modes: $\eta' K$, $\eta' K^*(892)$, $\eta' K_1(1270)$, $\eta' K_1(1400)$, $\eta' K^*(1410)$, $\eta' K_2^*(1430)$, $\eta' K_3^*(1780)$, and $\eta' K_4^*(2045)$. The efficiency discrepancy between the models and our knowledge of the resonant sector lead us to assign a 20% systematic uncertainty. Other systematic uncertainties include track reconstruction efficiency, reconstruction efficiencies of $\pi^0 \to \gamma\gamma$, $\eta \to \gamma\gamma$, and $K_S^0 \to \pi^+\pi^-$ candidates, charged-kaon identification efficiency, secondary branching fractions, number of $B\overline{B}$ events ($N_{B\overline{B}}$), the size of our Monte Carlo sample, and subtraction of the background from $\overline{B}^0 \to \eta' D^{(*)0}$.

To explore the X_s mass distribution, we select B candidates for which the mass of the η' is within 3 standard deviations of the known value and subtract the continuum contribution by using on-resonance data in the sideband $5.200 < m_{\rm ES} < 5.265$ GeV$/c^2$. The continuum background scaling factor ($\mathcal{A}$), from the sideband to signal

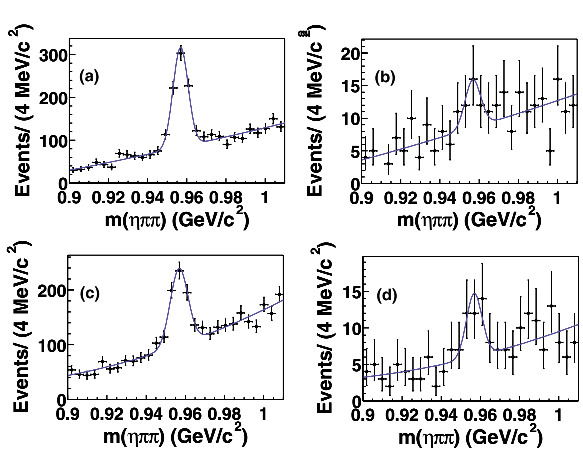

FIG. 2 (color online). Fits to the $\eta\pi\pi$ invariant mass for on-resonance (a),(c) and off-resonance (b),(d) data samples, for the modes (a),(b) $K^\pm$ and (c),(d) K_S^0.

TABLE II. Contribution of different sources to the systematic error for modes with a $K^{\pm}$ or K_S^0.

Source	$K^{\pm}$ syst (%)	K_S^0 syst (%)
Tracking	3.4	3.3
η, π^0 detection	7.0	8.2
K/K_S^0 ID	2.5	4.3
$\mathcal{B}(\eta' \to \eta_{\gamma\gamma}\pi\pi)$	3.4	3.4
$N_{B\overline{B}}$	1.1	1.1
MC sample size	3.0	3.0
$\eta' D^{(*)0}$ subtraction	3.0	2.9
Total	12.1	13.5
Model	20	20

regions, is computed from off-resonance data to be 0.591 ± 0.118. The resulting mass distributions are shown in Fig. 3 for all B modes and separately for the B^0 modes. The peak at $m(X_s) \simeq 500$ MeV$/c^2$ corresponds to the two body mode $B \to \eta' K$.

To obtain the full X_s spectrum, we fit the η' mass distribution in bins of X_s mass. The efficiency, averaged over the charged and neutral kaons, as a function of $m(X_s)$, is shown in Fig. 4. The correction for the feed across between bins is included in the efficiencies.

According to simulations, the X_s system is correctly reconstructed for 85% (60%) of the candidates in the region $m(X_s) < 1.5$ GeV$/c^2$ [$m(X_s) > 1.5$ GeV$/c^2$]. For correctly reconstructed events, the experimental resolution varies from 5 to 15 MeV$/c^2$ for low and high masses, respectively. In the case of misreconstructed events, the resolution ranges from 100 to 150 MeV$/c^2$. Table III shows the fitted yields for the raw signal, the sideband region, the expected color-suppressed background, and the yield after full background subtraction, as a function of $m(X_s)$.

The branching fraction as a function of $m(X_s)$, obtained from the fully background-subtracted yield (Table III), is shown in Fig. 5. We compare data and simulation by forming a χ^2 difference. The χ^2 probability for the nonresonant X_s model [Fig. 5(a)] to fit the data is 61%, while it is close to $\sim 10^{-7}$ for the equal mixture of resonances [Fig. 5(b)]. We find improved agreement with the resonant model if the weights of K_3^* and K_4^* are increased by a factor of 1.5, leading to a probability of 2%.

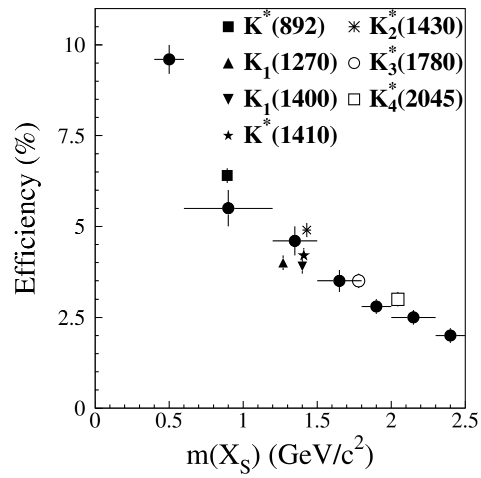

FIG. 4. Variation of the efficiency averaged over charged and neutral kaons with $m(X_s)$. The filled circles indicate the efficiency for nonresonant X_s simulation. The other symbols denote the values for the resonances.

As a consistency check of the method, we measure the two-body decay modes ($X_s = K^{\pm}, K_S^0$) and find 171.0 ± 14.0 and 27.1 ± 5.6 events in on-resonance data for $\eta' K^{\pm}$ and $\eta' K_S^0$, respectively, and no η' signal events for both channels in off-resonance data, leading to the branching fractions $\mathcal{B}(B^{\pm} \to \eta' K^{\pm}) = [6.9 \pm 0.6(\text{stat})] \times 10^{-5}$ and $\mathcal{B}(B^0 \to \eta' K^0) = [5.6 \pm 1.2(\text{stat})] \times 10^{-5}$. These values are fully compatible with what has been measured by recent exclusive analyses [12,13].

In summary, we have measured the branching fraction, $\mathcal{B}(B \to \eta' X_s) = [3.9 \pm 0.8(\text{stat}) \pm 0.5(\text{syst}) \pm 0.8(\text{model})] \times 10^{-4}$, for $2.0 < p^*(\eta') < 2.7$ GeV$/c$. We have also derived the $m(X_s)$ spectrum and found that the data tend to confirm models predicting a peak at high masses and seem to disfavor predictions based

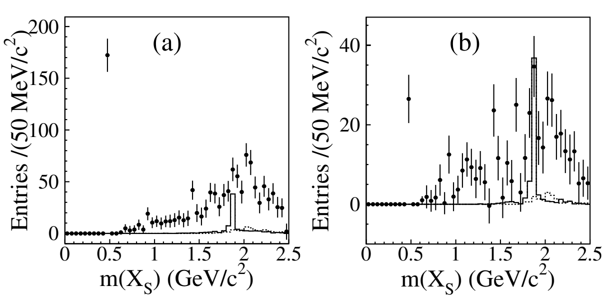

FIG. 3. Continuum-subtracted $Kn\pi$ invariant-mass distributions for (a) all B modes and (b) B^0 modes, including combinatorial background. Solid and dashed histograms represent expected backgrounds from $\overline{B}^0 \to \eta' D^0$ and $\overline{B}^0 \to \eta' D^{*0}$, respectively.

TABLE III. Fitted yields for on-resonance data and color-suppressed background for different $m(X_s)$ ranges in GeV$/c^2$. The sideband yields (Y_{SB}) must be corrected by the sideband to the signal region scaling factor (see text) before subtraction.

$m(X_s)$ range	Y_{ON}	Y_{SB}	Y_{CS}	Y
[0.4, 0.6]	200 ± 15	46.1 ± 8.8	$\cdots$	172.8 ± 15.9
[0.6, 1.2]	120 ± 14	100 ± 13	$\cdots$	60.9 ± 16.0
[1.2, 1.5]	114 ± 15	112 ± 14	1.1 ± 0.3	46.7 ± 17.1
[1.5, 1.8]	150 ± 18	163 ± 17	7.7 ± 1.6	46.0 ± 20.7
[1.8, 2.0]	140 ± 17	93 ± 15	47.4 ± 9.6	37.6 ± 21.4
[2.0, 2.3]	149 ± 20	142 ± 18	26.2 ± 4.5	38.9 ± 23.1
[2.3, 2.5]	80 ± 14	70 ± 14	4.9 ± 0.9	33.7 ± 16.3

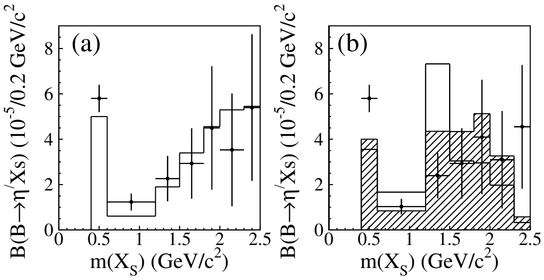

FIG. 5. Branching fractions as a function of $m(X_s)$. Both (a) and (b) show the same data, though the efficiency used in (a) is derived from the nonresonant model, while the efficiency in (b) comes from the model with a combination of resonances. The errors include bin-to-bin systematics; an additional systematic error of ~8% (not shown) is common to all points. (a) The open histogram represents the expectation from nonresonant $m(X_s)$ simulation. (b) The open histogram represents the expectation from a mixture of resonant modes with equal proportions. The hatched histogram results if some heavy resonances are enhanced.

only on the diagram of Figs. 1(a) and 1(b) for which $m(X_s)$ peaks near 1.4–1.5 GeV$/c^2$ [14].

Among the various theoretical conjectures to explain this production, an $\eta' gg$ coupling due to the QCD anomaly has been widely suggested as a likely explanation. However, the $\eta' gg$ form factor initially proposed [4] is disfavored by recent studies of the inclusive production $\Upsilon(1S) \to \eta' X$ [15,16]. A recently updated approach [6] exploiting the same η' gluon anomaly could in principle account for the observed branching fraction and the $m(X_s)$ spectrum.

We are grateful for the excellent luminosity and machine conditions provided by our PEP-II colleagues. The collaborating institutions wish to thank SLAC for its support and kind hospitality. This work is supported by DOE and NSF (USA), by NSERC (Canada), by IHEP (China), by CEA and CNRS-IN2P3 (France), by BMBF (Germany), by INFN (Italy), by NFR (Norway), by MIST (Russia), and by PPARC (United Kingdom). Individuals have received support from the Swiss NSF, A. P. Sloan Foundation, Research Corporation, and Alexander von Humboldt Foundation.

*Also with Università della Basilicata, Potenza, Italy.
†Also with IFIC, Instituto de Física Corpuscular, CSIC-Universidad de Valencia, Valencia, Spain.
‡Deceased.

[1] *BABAR* Collaboration, B. Aubert *et al.*, Phys. Rev. D **69**, 032004 (2004).
[2] *BABAR* Collaboration, B. Aubert *et al.*, hep-ex/0308015; Phys. Rev. Lett. **92**, 061801 (2004).
[3] CLEO Collaboration, Phys. Rev. Lett. **81**, 1786 (1998).
[4] D. Atwood and A. Soni, Phys. Lett. B **405**, 150 (1997).
[5] W. S. Hou and B. Tseng, Phys. Rev. Lett. **80**, 434 (1998).
[6] H. Fritzsch and Y-F. Zhou, Phys. Rev. D **68**, 034015 (2003).
[7] CLEO Collaboration, G. Bonvicini *et al.*, Phys. Rev. D **68**, 011101 (2003).
[8] *BABAR* Collaboration, B. Aubert *et al.*, Nucl. Instrum. Methods Phys. Res., Sect. A **479**, 1 (2002).
[9] G.C. Fox and S. Wolfram, Phys. Rev. Lett. **41**, 1581 (1978).
[10] Throughout this Letter, whenever a mode is given, the charge conjugate state is also implied.
[11] For off-resonance data, a rescaling is needed for $m_{\rm ES}$ to account for the center-of-mass energy difference.
[12] *BABAR* Collaboration, B. Aubert *et al.*, Phys. Rev. Lett. **91**, 161801 (2003).
[13] Belle Collaboration, K. Abe *et al.*, Phys. Lett. B **517**, 309 (2001).
[14] A. Datta *et al.*, Phys. Lett. B **419**, 369 (1998).
[15] A.L. Kagan, in *Heavy Flavor Physics: Ninth International Symposium on Heavy Flavor Physics, Pasadena, CA, 2001*, edited by Anders Ryd and Frank C. Porter, AIP Conf. Proc. No. 618 (AIP, Melville, NY, 2002), p. 310.
[16] CLEO Collaboration, M. Artuso *et al.*, Phys. Rev. D **67**, 052003 (2003).